

**Catalytic pathways identification for partial oxidation of methanol on copper-zinc catalysts:  $\text{CH}_3\text{OH} + 1/2\text{O}_2 \leftrightarrow \text{CO}_2 + 2\text{H}_2$**

11 September 2006

Yu-Chuan Lin <sup>1</sup>, L.T. Fan <sup>1,\*</sup>, Shahram Shafie <sup>1</sup>, Keith L. Hohn <sup>1</sup>,  
Botond Bertók <sup>2</sup>, Ferenc Friedler <sup>2</sup>

<sup>1</sup> Department of Chemical Engineering, Kansas State University,  
105 Durland Hall, Manhattan, KS 66506-5102, USA

<sup>2</sup> Department of Computer Science, University of Pannonia,  
Egyetem u. 10, Veszprem, H-8200, Hungary

---

\* To whom correspondence should be addressed. Tel: (785) 532-5584.

Fax: (785) 532-7372. E-mail: [fan@cheme.ksu.edu](mailto:fan@cheme.ksu.edu).

## 1. Introduction

Catalytic partial oxidation (CPO) of methanol yielding hydrogen has been extensively studied in the last decade [1-3] since hydrogen, by any measure, is an ultra clean fuel. This reaction offers the potential for converting a liquid fuel to hydrogen for use in the portable fuel cell system, which is popularly acknowledged as being a potential candidate to replace the internal combustion engine in vehicles [3,4]. Among the catalysts for this process, copper-zinc is the most prominent: it is active under moderate conditions (200~300°C) and generates relatively less CO than other catalysts. It is, therefore, not surprising that much effort has been expended to investigate CPO catalyzed by copper-zinc catalyst experimentally as well as theoretically [2,5,6].

A set of plausible elementary reactions has been proposed by Huang and Chren [5] for this catalytic reaction. It is mainly based on the mechanism hypothesized by Wachs and Madix [7]. According to the latter two, methanol molecules are chemisorbed on the copper-zinc surface, thereby forming methoxide. Subsequently, the methoxide groups interact among themselves as a dual-site reaction, thus generating formaldehyde and chemisorbed hydrogen. Eventually, gas phase hydrogen is released from the copper-zinc surface by another dual-site reaction among the chemisorbed hydrogen. Huang and Chren [5] have modified this mechanism by assuming the absence of chemisorbed hydrogen on the copper-zinc catalyst due to its low stability at room temperature; this hinders the production of hydrogen from the decomposition of methoxide and chemisorbed formaldehyde groups. Seven elementary reactions are included in this modified methanol CPO mechanism. If each of these elementary reactions is rewritten as a bimolecular reaction, the number of the elementary reactions in the set increases from 7 to 10. It is worth noting that Huang and Chern have not asserted that the set of elementary reactions proposed by them constitutes a stoichiometrically feasible mechanism or pathway.

The production of hydrogen from CPO of methanol has been extensively investigated experimentally; in contrast, relatively meager effort has been made to explore its catalytic mechanisms or pathways. The current work aims at the exhaustive generation of stoichiometrically feasible, independent catalytic pathways (IP<sub>i</sub>'s) of methanol's CPO from a set of plausible elementary

reactions by means of our graph-theoretic method based on P-graphs (process graph). This is followed by the derivation of a rate equation on the basis of each  $IP_i$  according to the Langmuir-Hishelwood-Hougen-Watson (LHHW) formalism [8,9]. The resultant rate equations are fitted to experimental data; the pathway corresponding to the best-fitting rate equation is deemed most likely to be the dominant or ultimate one. This identification of the dominant or ultimate pathway is greatly facilitated by various means, such as the spectroscopic determination of generation of active intermediate involved in the pathways of concern [10-12]. Obviously, the rate equation based on the dominant pathway would have practical utility in designing and operating industrial processes for implementing CPO of methanol.

## **2. Methodology**

### *2.1 Theoretical*

Presented herein are the graph-theoretic method based on P-graphs and the LHHW formalism. The former exhaustively identifies stoichiometrically feasible pathways for a given catalytic reaction, and the latter is for deriving the rate expressions on the basis of the resulting pathways, i.e., mechanisms.

#### *2.1.1 Graph-theoretic Method Based on P-graphs for Determining the Stoichiometrically Feasible Pathways*

The algorithms for implementing our graph-theoretic method based on P-graphs are rooted in two cornerstones. One is the two sets of axioms, including the six axioms of stoichiometrically feasible pathways, each consisting of elementary reactions, for any given overall reaction, and the seven axioms of combinatorially feasible networks of elementary reactions [10-12]. The other is the unambiguous representation of the networks of pathways by P-graphs, which are directed bipartite graphs. P-graphs comprise horizontal bars, which are the nodes representing an elementary-reaction steps, circles, which are the nodes representing biochemical or active species, and directed arcs linking these two types of nodes [13-15].

The aforementioned axioms and P-graphs representation give rise to three highly efficient algorithms necessary for synthesizing a stoichiometrically feasible pathway comprising elementary reactions. These three algorithms are

RPIMSG for maximal structure generation, RPISSG for solution-structure generation, and PBT for feasible-pathway generation. These algorithms have been successfully deployed to exhaustively identify catalytic and metabolic pathways for catalyzed chemical and biochemical reactions, respectively [10,12,16,17].

### *2.1.2 Derivation of Rate Equations according to LHHW Formalism*

The Langmuir-Hinshelwood-Hougen-Watson (LHHW) formalism offers an effective paradigm for deriving a surface-reaction kinetic model for heterogeneous catalytic reactions [18,19]. It takes into account all major physico-chemical phenomena involved in a heterogeneous catalytic reaction. Such phenomena include adsorption, surface reaction and desorption. In formulating the model, active sites on the surface of a catalyst are explicitly identified, thereby resulting in an active site balance [20].

The complexity and computational effort involved in deriving the rate equations according to the LHHW formalism can be minimized by various means. For instance, the stoichiometrically feasible IP<sub>i</sub>'s, in which the most abundant surface intermediates as identified by spectroscopy do not participate, are eliminated prior to the derivation.

## *2.2 Experimental*

### *2.2.1 Catalyst Preparation*

The catalyst comprising 40% of Cu supported on ZnO was prepared via the co-precipitation method [21,22]. The procedure was as follows: at the outset, aqueous solutions of two nitrate salts were prepared, one by dissolving 8.4 g of Cu(NO<sub>3</sub>)<sub>2</sub> into 300 mL of deionized water and the other by dissolving 13 g of Zn(NO<sub>3</sub>)<sub>2</sub> into the same amount of water. The mixture of these two solutions was fed dropwise into an aqueous solution of Na<sub>2</sub>CO<sub>3</sub> prepared by dissolving 10 g of Na<sub>2</sub>CO<sub>3</sub> also in 300 mL of deionized water. This mixture was then preheated to 80 °C with continuous stirring for 60 minutes. The resulting solution was then cooled to room temperature and filtered; the cake retained on the filter was ground and calcinated at 400 °C for 12 hours. The calcined cake in the form of powder was pelletized, crushed and sieved into particles between 40 to 45 mesh.

### 2.2.2 Measurements of Catalytic Activity

Experiments were performed in a vertical quartz-tube reactor inside a cylindrical furnace. Because of the high exothermicity of MPO, the catalyst bed was formed by blending 0.05 g of the Cu/ZnO catalyst with 0.45 g of SiO<sub>2</sub> (40 to 45 mesh). This bed was sandwiched between plugs of quartz wool. SiO<sub>2</sub>, inert under the experimental conditions, facilitated the dispersion of catalysts within the catalyst bed, thereby preventing the occurrence of hotspots. Prior to each experimental run, the catalyst bed was preheated from room temperature to 250 °C in a 4 °C/min ramp and maintained at 250 °C for an hour, during which a stream containing 30 mole% of H<sub>2</sub> and 70 mole% of N<sub>2</sub> was passed through it. The data were acquired via a gas chromatograph equipped with MollSeive 5A and Haysep T columns to separate the products. The details of measurements are available elsewhere [23]. Influences of internal and external mass transfer resistances were explored prior to the catalytic investigations. The internal resistance was examined by varying the catalysts' particle sizes. Two sizes of the particles were used; one ranged from 20 to 40 mesh, and the other ranged from 40 to 45 mesh. No difference was observed between the particle sizes. The external resistance was probed by changing the weight loading of the catalyst bed. Two loadings were selected; in one of the loadings, 0.03 g of catalyst was mixed with 0.37 g of SiO<sub>2</sub>, and in the other, 0.05 g of catalyst was mixed with 0.45 g of SiO<sub>2</sub>. No difference was observed between the two loadings.

## 3. Results and Discussion

### 3.1 Feasible IP<sub>i</sub>'s

Table 1 summarizes 13 elementary reactions, including 10 ( $s_1$  through  $s_{10}$ ) from the original set proposed by Huang and Chern [5] and 3 ( $s_{11}$  through  $s_{13}$ ) newly proposed by us, which can plausibly constitute the pathways or mechanisms of the CPO of methanol on Cu/ZnO catalyst. From these 13 elementary reactions, the current graph-theoretic approach based on P-graphs has generated 6 stoichiometrically feasible independent pathways (IP<sub>i</sub>'s), which are listed in Tables 2, within a second on a PC (Intel Pentium 4, CPU 3.06GHz; and 1G RAM). Note that Table 2 also contains the pathway proposed by Huang and Chern [5] as one of the IP<sub>i</sub>'s (IP<sub>5</sub>).

**Table 1. Elementary Reactions for the Oxidation of Methanol to Produce Hydrogen**

	Elementary Reactions
$s_1$	$O_2 + \ell \leftrightarrow O_2\ell$
$s_2$	$O_2\ell + \ell \leftrightarrow 2O\ell$
$s_3$	$CH_3OH + \ell \leftrightarrow CH_3OH\ell$
$s_4$	$CH_3OH\ell + O\ell \leftrightarrow CH_3O\ell + OH\ell$
$s_5$	$CH_3OH + OH\ell \leftrightarrow CH_3O\ell + H_2O$
$s_6$	$2CH_3O\ell \leftrightarrow 2CH_2O\ell + H_2$
$s_7$	$CH_2O\ell \leftrightarrow CO\ell + H_2$
$s_8$	$CO\ell \leftrightarrow CO + \ell$
$s_9$	$CO + O\ell \leftrightarrow CO_2 + \ell$
$s_{10}$	$H_2 + O\ell \leftrightarrow H_2O + \ell$
$s_{11}$	$H_2 + CH_2O\ell \leftrightarrow CH_3OH + \ell$
$s_{12}$	$CH_3OH + O\ell \leftrightarrow CH_2O\ell + H_2O$
$s_{13}$	$CH_2O\ell + OH\ell \leftrightarrow CH_3O\ell + O\ell$

**Table 2. Stoichiometrically Feasible Independent Pathways for Oxidation of Methanol to Produce Hydrogen**

Designation (IP <sub>i</sub> )	Mechanisms
IP <sub>1</sub>	$s_1 + s_2 + 2s_3 + 2s_4 + 2s_6 + 2s_7 + 2s_8 + 2s_9 + 2s_{13}$
IP <sub>2</sub>	$s_1 + s_2 + 2s_5 + 2s_7 + 2s_8 + 2s_9 - 2s_{10} - 2s_{13}$
IP <sub>3</sub>	$s_1 + s_2 + 2s_7 + 2s_8 + 2s_9 - 2s_{11}$
IP <sub>4</sub>	$s_1 + s_2 + 2s_7 + 2s_8 + 2s_9 - 2s_{10} + 2s_{12}$
IP <sub>5</sub>	$s_1 + s_2 + s_3 + s_4 + s_5 + s_6 + 2s_7 + 2s_8 + 2s_9 - s_{10}$
IP <sub>6</sub>	$s_1 + s_2 + 2s_3 + 2s_4 + 2s_5 + 2s_6 + 2s_7 + 2s_8 + 2s_9 - 2s_{12}$

### 3.2 Rate Equations

Methoxide has been known determined to be the most abundant surface intermediates in MPO on copper's surface [7,24]. Thus, IP<sub>3</sub> and IP<sub>4</sub>, not involving methoxide, have been eliminated. Table 3 lists the 12 rate equations obtained for the remaining 4 IP<sub>i</sub>'s, including IP<sub>1</sub>, IP<sub>2</sub>, IP<sub>5</sub> and IP<sub>6</sub>, derived according to the LHHW formalism. Specifically, the assumption that the adsorption, surface reaction or desorption step is rate-determining in each of the 4 IP<sub>i</sub>'s has given rise to these rate equations.

### 3.3 Parameter Estimation

Each of the rate equations for the remaining 4 IP<sub>i</sub>'s, i.e., IP<sub>1</sub>, IP<sub>2</sub>, IP<sub>5</sub>, and IP<sub>6</sub>, contains 4 parameters. When the adsorption step is rate-determining, they are  $k_{rd,i}$ ,  $K_{e,i}$ ,  $K_{sf,i}$  and  $K_{de,i}$ ; the surface reaction step,  $k_{rd,i}$ ,  $K_{ad,i}$ ,  $K_{e,i}$  and  $K_{de,i}$ ; the desorption step,  $k_{rd,i}$ ,  $K_{ad,i}$ ,  $K_{sf,i}$  and  $K_{e,i}$ . 3 sets of the 4 parameters include  $K_{e,i}$ ; however, its magnitude is inordinately large for MPO [5]. Thus, the term with  $K_{e,i}$  in the denominator can be regarded as negligibly small, thereby leaving 3 parameters to be estimated through the nonlinear regression of the four rate equations, listed in Table 3, on the experimental data. Specifically, nonlinear regression has been performed by resorting to an adoptive random search method subject to the criterion of the least residual sum of squares (RSS's) [25,26]. Table 3 summarizes the resultant values of the 3 parameters in the 12 rate equations derived from the 4 IP<sub>i</sub>'s. Among these 12 rate equations, those derived from IP<sub>2</sub>, IP<sub>5</sub>, and IP<sub>6</sub> by assuming that the surface-reaction step is rate-determining and those derived from IP<sub>1</sub> by assuming that the desorption step is rate-determining result in the lowest RSS. Moreover, the computed rates from the equations derived from IP<sub>2</sub>, IP<sub>5</sub> and IP<sub>6</sub> most closely follow the experimentally measured variational trend of the reaction rate as a function of the contact time. Nevertheless,  $K_{de,5}$  in the equation derived based on IP<sub>5</sub> is unusually large for the desorption step at equilibrium state. This, therefore, leaves only IP<sub>2</sub> and IP<sub>6</sub> as the potentially most dominant or ultimate pathways. Figure 1 compares the experimentally measured and estimated reaction rates for IP<sub>2</sub> and IP<sub>6</sub>. To discriminate between these two requires further exploration, such as in-situ spectroscopic studies [27] and reaction energetic analysis [28].

**Table 3. Rate Equations Derived for IP<sub>1</sub>, IP<sub>2</sub>, IP<sub>5</sub> and IP<sub>6</sub> and the Value of Parameters in the Equations.**

IP <sub>i</sub> 's	Adsorption (ad), surface reaction (sf) and desorption (de) steps. The rate-determining steps are marked with asterisk.	Derived rate equation	Fitted parameters
IP <sub>1</sub>	(ad): $O_2 + 2l \xrightleftharpoons{K_{e,1}} 2Ol$ *	$r_1 = \frac{k_{rd,1}O_2}{\left(1 + \frac{H_2CO_2}{K_{sf,1}K_{de,1}CH_3OH} + \frac{2H_2CO_2^{1/2}}{K_{de,1}^{1/2}}\right)^2}$	$k_{rd,1} = 4.6*10^5$ $K_{sf,1} = 8.7$ $K_{de,1} = 1.3*10^3$ $RSS = 1.1*10^{-4}$
	(sf): $CH_3OH + Ol + l \xrightleftharpoons{K_{sf,1}} CH_3Ol + OHl$		
	(de): $CH_3Ol + OHl \xrightleftharpoons{K_{de,1}} 2H_2 + CO_2 + l$		
IP <sub>1</sub>	(ad): $O_2 + 2l \xrightleftharpoons{K_{ad,1}} 2Ol$	$r_1 = \frac{k_{rd,1}K_{ad,1}O_2^{1/2}}{\left(1 + K_{ad,1}O_2^{1/2} + \frac{2H_2CO_2^{1/2}}{K_{de,1}^{1/2}}\right)^2}$	$k_{rd,1} = 5.9*10^{-2}$ $K_{ad,1} = 2.8*10^3$ $K_{de,1} = 2.5*10^{-14}$ $RSS = 7.1*10^{-5}$
	(sf): $CH_3OH + Ol + l \xrightleftharpoons{K_{e,1}} CH_3Ol + OHl$ *		
	(de): $CH_3Ol + OHl \xrightleftharpoons{K_{de,1}} 2H_2 + CO_2 + l$		
IP <sub>1</sub>	(ad): $O_2 + 2l \xrightleftharpoons{K_{ad,1}} 2Ol$	$r_1 = \frac{k_{rd,1}K_{ad,1}^{1/2}K_{sf,1}O_2^{1/2}CH_3OH}{\left(1 + K_{ad,1}^{1/2}O_2^{1/2} + 2K_{sf,1}^{1/2}K_{ad,1}^{1/4}O_2^{1/4}CH_3OH^{1/2}\right)^2}$	$K_{ad,1} = 4.4*10^5$ $K_{sf,1} = 8.0*10^{-1}$ $k_{rd,1} = 9.5*10^4$ $RSS = 2.4*10^{-5}$
	(sf): $CH_3OH + Ol + l \xrightleftharpoons{K_{sf,1}} CH_3Ol + OHl$		
	(de): $CH_3Ol + OHl \xrightleftharpoons{K_{e,1}} 2H_2 + CO_2 + l$ *		

**Table 3 (cont'd).**

IP <sub>i</sub> 's	Adsorption (ad), surface reaction (sf) and desorption (de) steps. The rate-determining steps are marked with asterisk.	Derived rate equation	Fitted parameters
	(ad): $O_2 + 2l \xleftarrow{K_{e,2}} 2Ol$ * (sf): $CH_3OH + Ol \xleftarrow{K_{sf,2}} CH_2Ol + H_2O$ (de): $2CH_2Ol + H_2O \xleftarrow{K_{de,2}} 2H_2 + CO_2 + l$	$r_2 = \frac{k_{rd,2} O_2}{\left(1 + \frac{H_2^2 CO_2}{K_{de,2} K_{sf,2} CH_3OH} + \frac{H_2^2 CO_2}{K_{de,2} H_2O}\right)^2}$	$k_{rd,2} = 4.6 \cdot 10^5$ $K_{sf,2} = 1.9$ $K_{de,2} = 2.4 \cdot 10^4$ RSS = $1.1 \cdot 10^{-4}$
IP <sub>2</sub>	(ad): $O_2 + 2l \xleftarrow{K_{ad,2}} 2Ol$ (sf): $CH_3OH + Ol \xleftarrow{K_{e,2}} CH_2Ol + H_2O$ * (de): $2CH_2Ol + H_2O \xleftarrow{K_{de,2}} 2H_2 + CO_2 + l$	$r_2 = \frac{k_{rd,2} K_{ad,2} O_2^{1/2} CH_3OH}{\left(1 + K_{ad,2} O_2^{1/2} + \frac{H_2^2 CO_2}{K_{de,2} H_2O}\right)}$	$k_{rd,2} = 6.4 \cdot 10^3$ $K_{ad,2} = 2.0 \cdot 10^5$ $K_{de,2} = 1.0 \cdot 10^{-11}$ RSS = $2.1 \cdot 10^{-5}$
	(ad): $O_2 + 2l \xleftarrow{K_{ad,2}} 2Ol$ (sf): $CH_3OH + Ol \xleftarrow{K_{sf,2}} CH_2Ol + H_2O$ (de): $2CH_2Ol + H_2O \xleftarrow{K_{e,2}} 2H_2 + CO_2 + l$ *	$r_2 = \frac{k_{rd,2} K_{ad,2}^{1/2} K_{sf,2} O_2^{1/2} CH_3OH}{1 + K_{ad,2}^{1/2} O_2^{1/2} + \frac{K_{ad,2}^{1/2} K_{sf,2} O_2^{1/2} CH_3OH}{H_2O}}$	$k_{rd,2} = 1.0 \cdot 10^6$ $K_{ad,2} = 4.0$ $K_{sf,2} = 2.7 \cdot 10^4$ RSS = $6.1 \cdot 10^{-5}$

**Table 3 (cont'd).**

IP <sub>i</sub> 's	Adsorption (ad), surface reaction (sf) and desorption (de) steps. The rate-determining steps are marked with asterisk.	Derived rate equation	Fitted parameters
	(ad): $O_2 + 2l \xrightleftharpoons{K_{e,5}} 2Ol$ * (sf): $2CH_3OH + Ol + l \xrightleftharpoons{K_{sf,5}} 2CH_3Ol + H_2O$ (de): $2CH_3Ol + 2H_2O \xrightleftharpoons{K_{de,5}} 5H_2 + 2CO_2 + 2l$	$r_5 = \frac{k_{rd,5}O_2}{\left(1 + \frac{H_2^5CO_2^2}{K_{sf,5}K_{de,5}^2H_2OCH_3OH^2} + \frac{H_2^{5/2}CO_2}{K_{de,5}H_2O}\right)^2}$	$k_{rd,5} = 4.6 \cdot 10^5$ $K_{sf,5} = 9.4 \cdot 10^{-1}$ $K_{de,5} = 4 \cdot 10^1$ $RSS = 1.1 \cdot 10^{-4}$
IP <sub>5</sub>	(ad): $O_2 + 2l \xrightleftharpoons{K_{ad,5}} 2Ol$ (sf): $2CH_3OH + Ol + l \xrightleftharpoons{K_{e,5}} 2CH_3Ol + H_2O$ * (de): $2CH_3Ol + 2H_2O \xrightleftharpoons{K_{de,5}} 5H_2 + 2CO_2 + 2l$	$r_5 = \frac{k_{rd,5}K_{ad,5}O_2^{1/2}CH_3OH^2}{\left(1 + K_{ad,5}O_2^{1/2} + \frac{H_2^{5/2}CO_2}{K_{de,5}H_2O}\right)^3}$	$k_{rd,5} = 2.4 \cdot 10^{10}$ $K_{ad,5} = 5.6 \cdot 10^3$ $K_{de,5} = 1.1 \cdot 10^1$ $RSS = 2.3 \cdot 10^{-5}$
	(ad): $O_2 + 2l \xrightleftharpoons{K_{ad,5}} 2Ol$ (sf): $2CH_3OH + Ol + l \xrightleftharpoons{K_{sf,5}} 2CH_3Ol + H_2O$ (de): $2CH_3Ol + 2H_2O \xrightleftharpoons{K_{e,5}} 5H_2 + 2CO_2 + 2l$ *	$r_5 = \frac{k_{rd,5}K_{ad,5}^{1/2}K_{sf,5}O_2^{1/2}CH_3OH^2H_2O}{\left(1 + K_{ad,5}^{1/2}O_2^{1/2} + \frac{K_{ad,5}^{1/4}K_{sf,5}^{1/2}O_2^{1/4}CH_3OH}{H_2O^{1/2}}\right)^2}$	$k_{rd,5} = 2.8 \cdot 10^2$ $K_{sf,5} = 3.5 \cdot 10^{10}$ $K_{de,5} = 1.3 \cdot 10^{10}$ $RSS = 2.2 \cdot 10^{-4}$

**Table 3 (cont'd).**

IP <sub>i</sub> 's	Adsorption (ad), surface reaction (sf) and desorption (de) steps. The rate-determining steps are marked with asterisk.	Derived rate equation	Fitted parameters
	(ad): $O_2 + 2l \xrightarrow{K_{e,6}} 2Ol$ * (sf): $2CH_3OH + Ol + l \xrightarrow{K_{sf,6}} 2CH_3Ol + H_2O$ (de): $2CH_3Ol + H_2O \xrightarrow{K_{de,6}} CH_3OH + 2H_2 + CO_2 + 2l$	$r_6 = \frac{k_{rd,6}O_2}{\left(1 + \frac{H_2CO_2}{K_{sf,6}K_{de,6}CH_3OH} + \frac{CH_3OH^{1/2}H_2CO_2^{1/2}}{K_{de,6}^{1/2}H_2O^{1/2}}\right)^2}$	$k_{rd,6} = 4.6 \cdot 10^5$ $K_{sf,6} = 5.9$ $K_{de,6} = 6.2 \cdot 10^5$ $RSS = 1.1 \cdot 10^{-4}$
IP <sub>6</sub>	(ad): $O_2 + 2l \xrightarrow{K_{ad,6}} 2Ol$ (sf): $2CH_3OH + Ol + l \xrightarrow{K_{e,6}} 2CH_3Ol + H_2O$ * (de): $2CH_3Ol + H_2O \xrightarrow{K_{de,6}} CH_3OH + 2H_2 + CO_2 + 2l$	$r_6 = \frac{k_{rd,6}K_{ad,6}O_2^{1/2}CH_3OH^2}{\left(1 + K_{ad,6}O_2^{1/2} + \frac{CH_3OH^{1/2}H_2CO_2^{1/2}}{K_{de,6}H_2O^{1/2}}\right)^2}$	$k_{rd,6} = 1.4 \cdot 10^{10}$ $K_{ad,6} = 1.1 \cdot 10^4$ $K_{de,6} = 3.7 \cdot 10^{-8}$ $RSS = 2.1 \cdot 10^{-5}$
	(ad): $O_2 + 2l \xrightarrow{K_{ad,6}} 2Ol$ (sf): $2CH_3OH + Ol + l \xrightarrow{K_{sf,6}} 2CH_3Ol + H_2O$ (de): $2CH_3Ol + H_2O \xrightarrow{K_{e,6}} CH_3OH + 2H_2 + CO_2 + 2l$ *	$r_6 = \frac{k_{rd,6}K_{ad,6}^{1/2}K_{sf,6}O_2^{1/2}CH_3OH^2}{\left(1 + K_{ad,6}^{1/2}O_2^{1/2} + \frac{K_{ad,6}^{1/4}K_{sf,6}^{1/2}O_2^{1/4}CH_3OH}{H_2O^{1/2}}\right)^2}$	$k_{rd,6} = 3.2 \cdot 10^5$ $K_{sf,6} = 8.9 \cdot 10^8$ $K_{de,6} = 1.3 \cdot 10^4$ $RSS = 1.4 \cdot 10^{-4}$

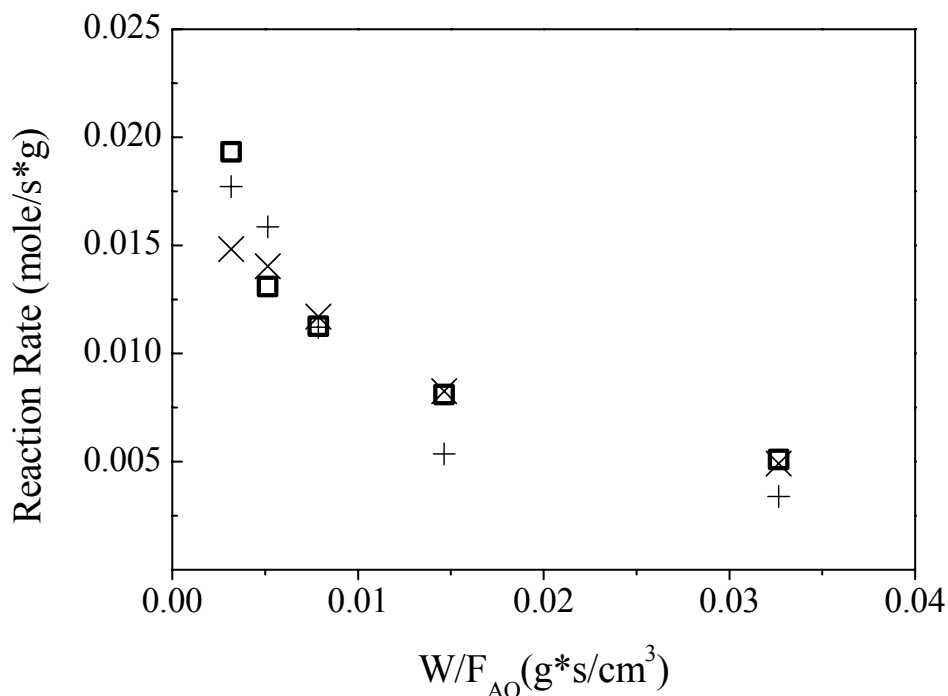


Figure 1. Comparison between the experimentally measured and estimated reaction rates for IP<sub>2</sub> and IP<sub>6</sub>: □, experimentally data; ×, estimated values for IP<sub>2</sub>; and +, estimated values for IP<sub>6</sub>.

#### 4. Concluding Remarks

The stoichiometrically feasible pathways of MPO have been exhaustively identified in a short time by using the graph-theoretic method based on P-graphs. The rate equations of these pathways have been derived according to the LHHW formalism. Subsequently, the rate constants of these equations have been estimated through the non-linear regression of the equations on the available experimental data. Two potentially dominant pathways have been determined based on the least-square criterion.

The current work ushers in a novel paradigm for determining the pathway of a catalytic reaction, initiating the rigorous graph-theoretic and exhaustive identification of stoichiometrically feasible independent pathways at the outset, followed by theoretical, mechanistic, computational and/or experimental exploration of the reaction on the basis of such pathways.

## Acknowledgements

The authors acknowledge Andres Argoti at Department of Chemical Engineering, Kansas State University for his assistance in conducting nonlinear regression by the adoptive random search method. This work was supported by Army Research Office under Grant No. DAAD 19-03-1-0100.

## Notation

$IP_i$	independent pathway
$k_{rd,i}$	forward rate constant of surface reaction of pathway i
$K_{ad,i}$	equilibrium constant of adsorption of pathway i
$K_{eq,i}$	equilibrium constant of surface reaction of pathway i
$K_{de,i}$	equilibrium constant of desorption of pathway i
LHHW	Langmuir-Hishelwood-Hougen-Watson
MPO	methanol partial oxidation
PBT	pathway-back-tracking
RPIMSG	algorithm of reaction pathway identification of maximum structure generation
RPISSG	algorithm of reaction pathway identification of solution structure generation
RSS	residual sum of squares

## Literature Cited

- [1] Mallen, M.P. Zum, Schmidt, L.D., (1996) Oxidation of methanol over polycrystalline Rh and Pt: rate, OH desorption, and model. *Journal of Catalysis*, 161, 230-246.
- [2] Velu, S., Suzuki, K., Osaki, T., (1999). Selective production of hydrogen by partial oxidation of methanol over catalysts derived from CuZnAl-layered double hydroxides. *Catalysis Letters*, 62, 159-167.
- [3] Agrell, J., Bigeresson, H., Boutonnet, M., Melián-Cabrera, I., Navarro, R.M., Fierro, J.L.G., (2003). Production of hydrogen from methanol over Cu/ZnO catalysts promoted by ZrO<sub>2</sub> and Al<sub>2</sub>O<sub>3</sub>. *Journal of Catalysis*, 219, 389-403.
- [4] Li, Y., Fu, Q., Flytzani-Stephanopoulos, M., (2000). Low-temperature water-gas shift reaction over Cu- and Ni-loaded cerium oxide catalysts. *Applied Catalysis B*, 27, 179-191.
- [5] Huang, T.J., Chren S.L., (1988). Kinetics of partial oxidation of methanol over a copper-zinc catalyst. *Applied Catalysis*, 40, 43-52.
- [6] Sakong, S., Groß, A., (2005). Density functional theory study of the partial oxidation of methanol on copper surfaces. *Journal of Catalysis*, 231, 420-429.
- [7] Wachs, I.E., Madix, R.J., (1978). The selective oxidation of CH<sub>3</sub>OH to H<sub>2</sub>CO on a copper (1 1 0) catalyst. *Journal of Catalysis*, 53, 208-227.
- [8] Hougen, O.A., Watson, K.M., (1943). Solid catalysts and reaction rates. *Industrial and Engineering Chemistry*, 35, 529-541.
- [9] Carberry, J.J. (1976). *Chemical and Catalytic Reaction Engineering*, 3<sup>rd</sup> edition, McGraw-Hill, New York, pp. 382-388.
- [10] Fan, L.T., Bertók, B., Friedler, F., Shafie, S., (2001). Mechanisms of ammonia-synthesis reaction revisited with the aid of a novel graph-theoretic method for determining candidate mechanisms in deriving the rate law of a catalytic reaction. *Hungarian Journal of Industrial Chemistry*, 29, 71-80.
- [11] Fan, L.T., Bertók, B., Friedler, F., (2002). A graph-theoretic method to identify candidate mechanisms for deriving the rate law of a catalytic reaction. *Computers and Chemistry*, 26, 265-292.
- [12] Fan, L.T., Shafie, S., Bertók, B., Friedler, F., Lee, D.Y., Seo, H., Park, S., Lee, S.Y., (2005). Graph-theoretic approach for identifying catalytic or metabolic pathways. *Journal of the Chinese Institute of Engineers*, 28, 1021-1037.

- [13] Friedler, F., Tarjan, K., Huang, Y.W., Fan, L.T., (1992). Combinatorial algorithms for process synthesis. *Chemical Engineering Science*, 47, 1973-1988.
- [14] Friedler, F., Tarjan, K., Huang, Y.W., Fan, L.T., (1993). Graph-theoretic approach to process synthesis: polynomial algorithm for maximal structure generation. *Computers Chemical Engineering*, 17, 929-942.
- [15] Friedler, F., Varga, J.B., Fan, L.T., (1995). Decision-mapping: a tool for consistent and complete decision in process synthesis. *Chemical Engineering Science*, 50, 1755-1768.
- [16] Seo, H., Lee, D.Y., Park, S., Fan, L.T., Shafie, S., Bertók, B., Friedler, F., (2001). Graph-theoretical identification of pathways for biochemical reactions. *Biotechnology Letters*, 23, 1551-1557.
- [17] Lee, D.Y., Fan, L.T., Park, S., Lee, S.Y., Shafie, S., Bertók, B., Friedler, F., (2005). Complementary identification of multiple flux distributions and multiple metabolic pathways. *Metabolic Engineering*, 7, 182-200.
- [18] Balakos, M.W., Chuang, S.S.C., (1995). Dynamic and LHHW kinetic analyses of heterogeneous catalytic hydroformylation. *Journal of Catalysis*, 151, 266-278.
- [19] Brundage, M.A., Balakos, M.W., Chuang, S.S.C., (1998). LHHW and PSSA kinetic analysis of rates and adsorbate coverages in CO/H<sub>2</sub>/C<sub>2</sub>H<sub>4</sub> reaction on Mn-Rh/SiO<sub>2</sub>. *Journal of Catalysis*, 173, 122-133.
- [20] Fogler, H.S. (1999). *Elements of Chemical Reaction Engineering*; Prentice-Hall: New Jersey.
- [21] Reitz, T.L., Lee, P.L., Czaplewski, K.F., Lang, J.C., Popp, K.E., Kung, H.H., (2001). Time-resolved XANES investigation of CuO/ZnO in the oxidative methanol reforming reaction. *Journal of Catalysis*, 199, 193-201.
- [22] Schrum, E.D., Reitz, T.L., Kung, H.H., (2001). Deactivation of CuO/ZnO and CuO/ZrO<sub>2</sub> catalysts for oxidative methanol reforming. *Studies in Surface Science and Catalysis*, 139, 229-235.
- [23] Lin, Y.C., Hohn, K.L., (2006). Effect of sol-gel synthesis on physical and chemical properties of V/SiO<sub>2</sub> and V/MgO catalysts. *Catalysis Letters*, 107, 215-222.
- [24] Millar, G.J., Rochester, C.H., Waugh, K.C., (1992). Evidence for the adsorption of molecules at special sites located at copper/zinc oxide interfaces. *Journal of the Chemical Society. Faraday Transactions*, 88, 2257-2261.
- [25] Fan, L.T., Chen, H.T., Aldis, D., (1975). An adoptive random search procedure for large scale industrial and process systems synthesis. In:

Proceeding of Symposium on Computers in the Design and Erection of Chemical Plants, pp. 279-291.

- [26] Chen, H.T., Fan, L.T., (1976). Multiple minima in a fluidized reactor-heater system. *AIChE Journal*, 22, 680-685.
- [27] Weckhuysen, B.M., (2002). Snapshot of a working catalyst: possibilities and limitation of in situ spectroscopy in the field of heterogeneous catalysis. *Chemical Communication*, 2, 97-110.
- [28] Nakamura, J., Campbell, J.M., Campbell, C.T., (1990). Kinetics and mechanism of the water-gas shift reaction catalysed by the clean and Cs-promoted Cu (1 1 0) surface: a comparison with Cu (1 1 1). *Journal of the Chemical Society. Faraday Transactions*, 86, 2725-2734.